Supplementary information

Highly luminescent and photoconductive columnar liquid crystals with a thiophene-oxadiazole backbone

Konstantin Iakoubovskii*[1] and Masafumi Yoshio*[,1,2]

1 Research Center for Macromolecules & Biomaterials, National Institute for Materials Science, 1-2-1 Sengen, Tsukuba, Ibaraki 305-0047, Japan.

2 Graduate School of Chemical Sciences and Engineering, Hokkaido University, Kita 13, Nishi 8, Kita-ku, Sapporo, Hokkaido 060-8628, Japan.

*E-mail: IAKOUBOVSKII.Konstantin@nims.go.jp

*E-mail: YOSHIO.Masafumi@nims.go.jp

Contents

1. General methods

^{1}H and ^{13}C nuclear magnetic resonance (NMR) spectra were recorded with a JEOL JNM–AL30/BZ spectrometer at 400 and 100 MHz, respectively. The chemical shifts (δ) of ^{1}H and ^{13}C NMR signals were reported in ppm and referenced to residual solvents of CD_2Cl_2 (^{1}H = 5.32 ppm; ^{13}C = 53.84 ppm) and $CDCl_3$ (^{1}H = 7.26 ppm; ^{13}C = 77.00 ppm), or tetramethylsilane (δ = 0.00) as an internal standard for $CDCl_3$ solutions. Matrix-assisted laser desorption/ionization time-of-flight mass spectroscopy (MALDI TOF-MS) was conducted with a Shimadzu AXIMA-CFR Plus setup using dithranol as a matrix. Elemental analysis for C, H, N, and S was carried out by using an ELEMENTAR vario EL cube. Optical photographs were taken with an Olympus BX51N-31P-O3 microscope equipped with a DP22 digital camera and a LINKAM T95-HS, LTS420E temperature control system; the observed sample was placed between crossed polarizers. Differential scanning calorimetry (DSC) measurements were carried out under a continuous argon purge (40 mL/min) using a NETZSCH DSC-3500 Sirius system. The heating and cooling rates were 10 °C/min. X-ray diffraction patterns were recorded with a Rigaku MiniFlex 600 diffractometer using Ni-filtered Cu Kα radiation. UV-visible absorption was measured with a Jasco V-750 spectrometer.

2. Materials

Methyl gallate, 1-bromododecane, 1-bromodecane, 4-bromobenzoyl chloride, and 2,2'-bithiphene-5,5'-diboronic acid bis(pinacol ester) were purchased from Tokyo Chemical Industry. Hydrazine monohydrate, triethylamine (TEA), potassium carbonate, anhydrous magnesium sulfate, sodium carbonate, anhydrous tetrahydrofuran (THF), hexane, chloroform, ethyl acetate (EtOAc), and ethanol (EtOH) were purchased from Kanto Chemical. Phosphorous oxychloride ($POCl_3$) and anhydrous dichloromethane were purchased from Wako. Tetrakis(triphenylphosphine)palladium(0) ($Pd(PPh_3)_4$) was purchased from Sigma–Aldrich.

3. Synthesis

Compounds **1a,b** were synthesized according to Scheme S1. Methyl 3,4,5-tris(dodecyloxy)benzoate (**2a**), methyl 3,4,5-tris(decyloxy)benzoate (**2b**), 3,4,5-tris(dodecyloxy)benzohydrazide (**3a**), and 3,4,5-tris(decyloxy)benzohydrazide (**3b**) were synthesized according to the reported procedures.[S1]

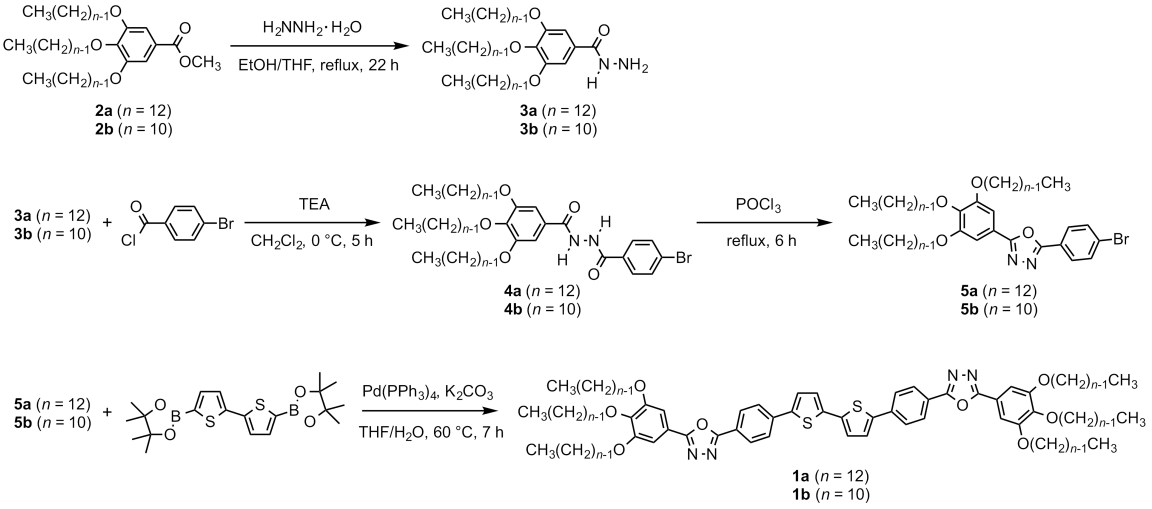

Scheme 1. Synthesis of hexacatenar oligothiophene-oxadiazole conjugates.

N-(4-bromobenzoyl)-3,4,5-tris(dodecyloxy)benzohydrazide (**4a**).

To a solution of **3a** (2.07 g, 3.01 mmol) in TEA (2 mL) and CH_2Cl_2 (30 mL), 4-bromobenzoyl chloride (0.726 g, 3.31 mmol) dissolved in 10 mL CH_2Cl_2 was added dropwise at 0 °C. The reaction mixture was stirred for 5 h. The white precipitate was obtained by filtration and washed with water and methanol. The solid was dissolved in $CHCl_3$ and the solution was dried over anhydrous $MgSO_4$. After filtration and evaporation, the product was purified by silica gel column chromatography (eluent: hexane/$CHCl_3$ = 7/3–0/10, vol./vol.) to afford **4a** (1.88 g, 2.16 mmol, 72%) as a white solid. ^{1}H NMR ($CDCl_3$, 400 MHz): 10.59 (d, *J* = 3.2 Hz, 1H), 10.00 (d, *J* = 2.8 Hz, 1H), 7.70 (d, *J* = 8.8 Hz, 2H), 7.45 (d, *J* = 8.8 Hz, 2H), 7.02 (s, 2H), 3.98–3.68 (m, 6H), 1.76–1.71 (m, 6H), 1.40–1.26 (m, 54H), 0.88 (t, J = 6.4 Hz, 9H). ^{13}C NMR ($CDCl_3$, 100 Hz): 165.13, 164.96, 153.07, 141.74, 131.64, 129.80, 128.98, 127.12, 125.46, 105.63, 73.46, 69.08, 31.92, 30.36, 29.74, 29.68, 29.61, 29.48, 29.38, 26.10, 22.68, 14.09. MALDI-TOF (positive ion, reflection mode): *m/z* calculated for $C_{50}H_{83}BrN_2O_5Na$ $[M+Na]^+$, 893.54; found 893.89. Elemental analysis calculated for $C_{50}H_{83}BrN_2O_5$: C, 68.86; H, 9.59; N, 3.21%; found: C, 69.20; H, 9.23; N, 2.92%.

N-(4-Bromobenzoyl)-3,4,5-tris(decyloxy)benzohydrazide (**4b**).

Synthesized from **3b** (3.15 g, 5.21 mmol) and 4-bromobenzoyl chloride (1.26 g, 5.73 mmol). Yield 2.68 g (3.40 mmol, 65 %). ^{1}H NMR ($CDCl_3$, 400 MHz): 10.13 (s, 1H), 9.69 (s, 1H), 7.72 (d, *J* = 8.4 Hz, 2H), 7.51 (d, *J* = 8.4 Hz, 2H), 7.04 (s, 2H), 3.98 (t, *J* = 6.4 Hz, 2H), 3.92 (t, *J* = 6.4 Hz, 4H), 1.80–1.70 (m, 6H), 1.51–1.39 (m, 6H), 1.36–1.20 (m, 36H), 0.88 (t, *J* = 6.6 Hz, 9H). ^{13}C NMR ($CDCl_3$, 100 MHz): 165.53, 164.38, 153.17, 141.85, 131.83, 129.93, 128.91, 127.23, 125.56, 105.64, 73.50, 69.18, 31.91, 30.34, 29.74, 29.64, 29.60, 29.43, 29.37, 26.08, 22.68, 14.10. Elemental analysis calculated for $C_{44}H_{71}BrN_2O_5$: C, 67.07; H, 9.08; N, 3.56%; found: C, 67.21; H, 8.67; N, 3.20%.

2-(4-Bromophenyl)-5-[3,4,5-tris(dodecyloxy)phenyl]-1,3,4-oxadiazole (**5a**).

A mixture of **4a** (2.92 g, 3.34 mmol) and $POCl_3$ (16 mL, 165 mmol) was refluxed for 6 h. All volatiles were removed in vacuo. The residue was dissolved in $CHCl_3$ and washed with a Na_2CO_3 aq. solution. The combined organic phase was dried over $MgSO_4$. After filtration and evaporation, the crude product was purified by silica gel column chromatography (eluent: hexane/$CHCl_3$ = 10/0–2/8) to give **5a** (2.16 g, 2.52 mmol, 75%) as a white solid. ^{1}H NMR ($CDCl_3$, 400 MHz): 8.00 (d, *J* = 8.8 Hz, 2H), 7.67 (d, *J* = 8.4 Hz, 2H), 7.30 (s, 2H), 4.09–4.03 (m, 6H), 1.87–1.77 (m, 6H), 1.52–1.49 (m, 6H), 1.43–1.20 (m, 48H), 0.88 (t, *J* = 6.4 Hz, 9H). ^{13}C NMR ($CDCl_3$, 100 MHz): 164.87, 163.61, 153.58, 141.48, 132.34, 128.24, 126.25, 122.85, 118.21, 105.41, 73.59, 69.36, 31.90, 30.32, 29.68, 29.62, 29.56, 29.38, 29.35, 29.30, 26.06, 22.66, 14.08. MALDI-TOF (positive ion, reflection mode): *m/z* calculated for $C_{50}H_{82}BrN_2O_4$ $[M + H]^+$, 855.54; found 855.49. Elemental analysis calculated for $C_{50}H_{81}BrN_2O_4$: C, 70.31; H, 9.56; N, 3.28%; found: C, 70.66; H, 9.17; N, 3.23%.

2-(4-Bromophenyl)-5-[3,4,5-tris(decyloxy)phenyl]-1,3,4-oxadiazole (**5b**).

Synthesized from **4b** (1.98 g, 2.52 mmol) and $POCl_3$ (16 mL, 165 mmol). Yield 1.43 g (1.86 mmol, 74 %) as a white solid. ^{1}H NMR ($CDCl_3$, 400 MHz): 8.00 (d, *J* = 8.8 Hz, 2H), 7.67 (d, *J* = 8.4 Hz, 2H), 7.30 (s, 2H), 4.09–4.03 (m, 6H), 1.87–1.77 (m, 6H), 1.52–1.49 (m, 6H), 1.43–1.20 (m, 36H), 0.88 (t, *J* = 6.4 Hz, 9H). ^{13}C NMR ($CDCl_3$, 100 MHz): 164.87, 163.61, 153.58, 141.48, 132.34, 128.24, 126.25, 122.85, 118.21, 105.41, 73.59, 69.36, 31.90, 30.32, 29.68, 29.62, 29.56,

29.38, 29.35, 29.30, 26.06, 22.66, 14.08. Elemental analysis calculated for $C_{44}H_{69}BrN_2O_4$: C, 68.64; H, 9.03; N, 3.64%; found: C, 67.69; H, 8.80; N, 3.19%.

Hexacatenar molecule with dodecyloxy chains (**1a**).

A mixture of **5a** (481 mg, 0.564 mmol), 2,2'-bithiphene-5,5'-diboronic acid bis(pinacol ester) (113 mg, 0.269 mmol), and K_2CO_3 (778 mg, 5.64 mmol) in 10 mL of tetrahydrofuran (THF) and 5 mL of H_2O was deaerated by bubbling of Ar gas. $Pd(PPh_3)_4$ (65.1 mg, 0.0563 mmol) was added to the mixture, which was stirred at 60 °C for 7 h. After the evaporation of the solvent, $CHCl_3$ was added and washed with water. The organic layer was dried over anhydrous $MgSO_4$, filtered, and evaporated. The residue was purified by flash column chromatography on silica gel (gradient from eluent: hexane/$CHCl_3$ = 5/5 to hexane/$CHCl_3$ = 7/3) and recrystallization from EtOAc/MeOH to afford **1** as an orange solid (370 mg, 0.216 mmol, 80 %). ^{1}H NMR (CD_2Cl_2, 400 MHz): 8.14 (d, *J* = 8.8 Hz, 4H), 7.78 (d, *J* = 8.8 Hz, 4H), 7.43 (d, *J* = 4.0 Hz, 2H), 7.32 (s, 4H), 7.28 (d, *J* = 4.4 Hz, 2H), 4.09 (t, *J* = 6.4 Hz, 8H), 4.02 (t, *J* = 6.8 Hz, 4H), 1.89–1.71 (m, 12H), 1.56–1.43 (m, 12H), 1.42–1.20 (m, 96H), 0.88 (t, *J* = 6.6 Hz, 18H). ^{13}C NMR (CD_2Cl_2, 100 MHz): 165.06, 164.37, 154.04, 142.28, 141.63, 138.01, 137.15, 127.74, 126.14, 125.70, 125.54, 123.22, 118.86, 105.44, 73.95, 69.73, 32.37, 30.79, 30.16, 30.10, 30.02, 29.88, 29.81, 26.55, 23.12, 14.30. MALDI-TOF (positive ion, reflection mode): *m/z* calculated for $C_{108}H_{167}N_4O_8S_2$ $[M + H]^+$, 1713.22; found 1713.01. Elemental analysis calculated for $C_{108}H_{166}N_4O_8S_2$: C, 75.74; H, 9.77; N, 3.27; S, 3.74%; found: C, 76.18; H, 9.36; N, 2.96; S, 4.13%.

Hexacatenar molecule with decyloxy chains (**1b**).

Synthesized from **5b** (0.607 g, 0.788 mmol), 2,2'-bithiphene-5,5'-diboronic acid bis(pinacol ester) (157 mg, 0.375 mmol), K_2CO_3 (1.09 g, 7.88 mmol), and $Pd(PPh_3)_4$ (91.3 mg, 0.079 mmol). Yield 0.517 g (0.335 mmol, 89 %) as an orange solid. ^{1}H NMR (CD_2Cl_2, 400 MHz): 8.14 (d, *J* = 8.8 Hz, 4H), 7.78 (d, *J* = 8.4 Hz, 4H), 7.42 (d, *J* = 3.6 Hz, 2H), 7.32 (s, 4H), 7.28 (d, *J* = 3.6 Hz, 2H), 4.09 (t, *J* = 6.4 Hz, 8H), 4.02 (t, *J* = 6.8 Hz, 4H), 1.89–1.71 (m, 12H), 1.56–1.43 (m, 12H), 1.42–1.20 (m, 72H), 0.89 (t, 6.8 Hz, 18H). ^{13}C NMR (CD_2Cl_2, 100 MHz): 164.95, 164.27, 153.98, 142.14, 141.56, 137.95, 137.00, 127.62, 125.96, 125.56, 125.40, 123.11, 118.83, 105.36, 73.91, 69.70, 32.38, 30.83, 30.21, 30.13, 30.08, 29.93, 29.83, 26.57, 23.14, 14.32. Elemental analysis calculated for $C_{96}H_{142}N_4O_8S_2$: C, 74.66; H, 9.27; N, 3.63; S, 4.15%; found: C, 75.07; H, 8.80; N, 3.32; S, 4.42%.

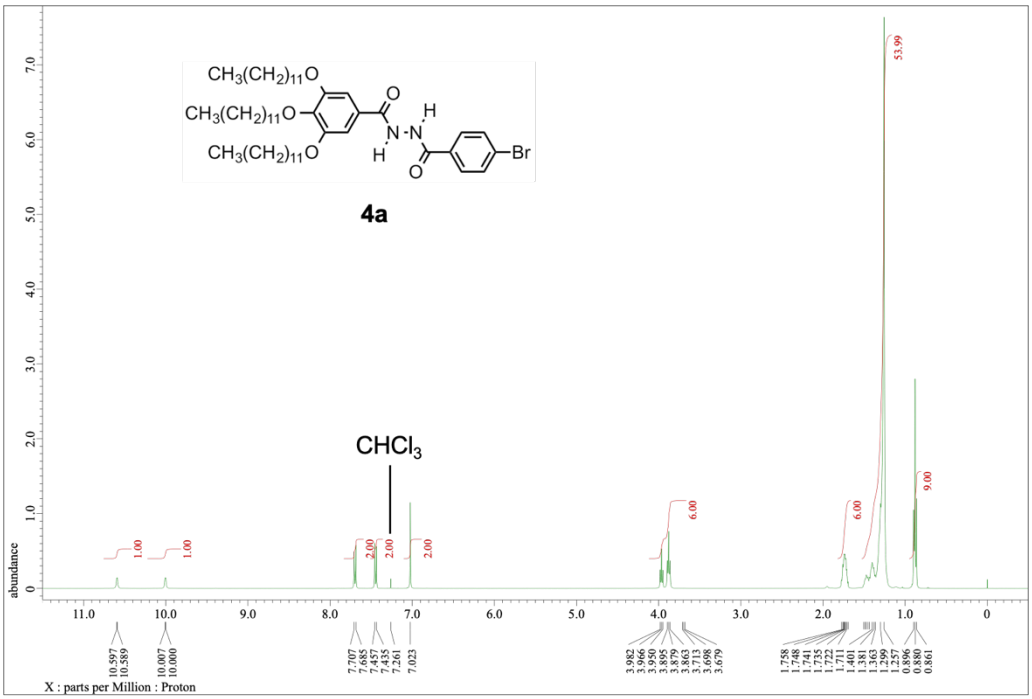

Figure S1. ^{1}H NMR spectrum of **4a** in $CDCl_3$ at 298 K.

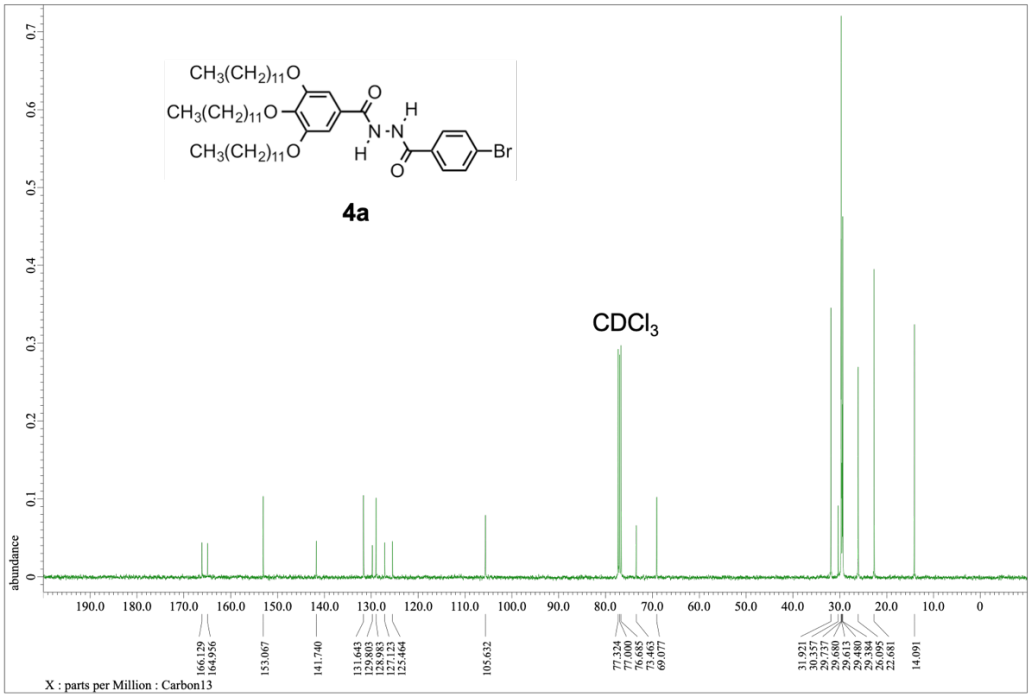

Figure S2. ^{13}C NMR spectrum of **4a** in $CDCl_3$ at 298 K.

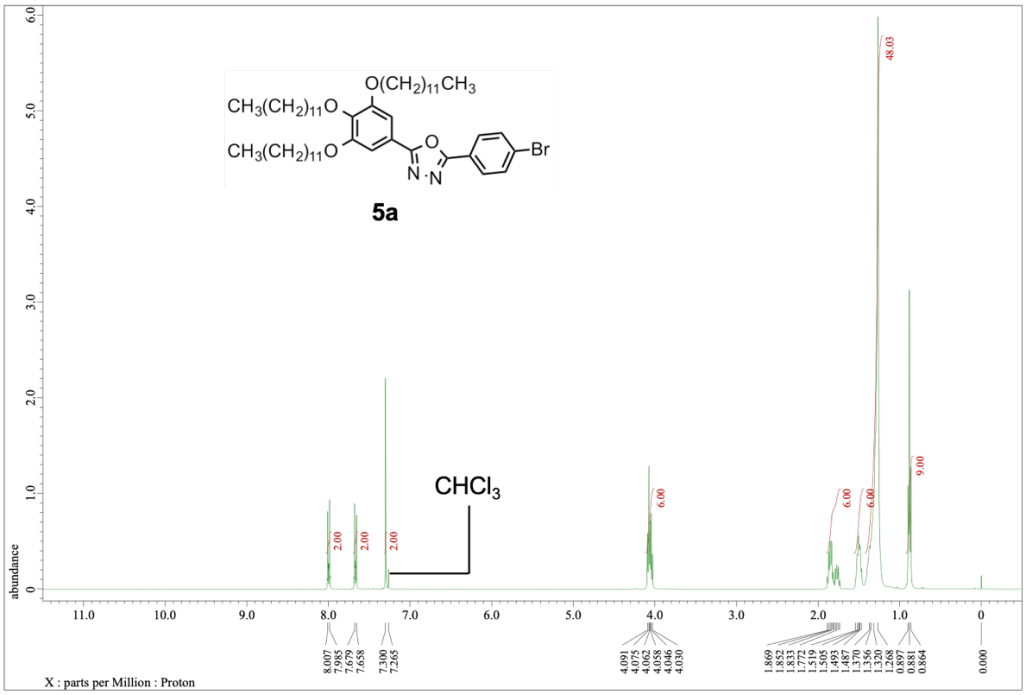

Figure S3. ^{1}H NMR spectrum of **5a** in $CDCl_3$ at 298 K.

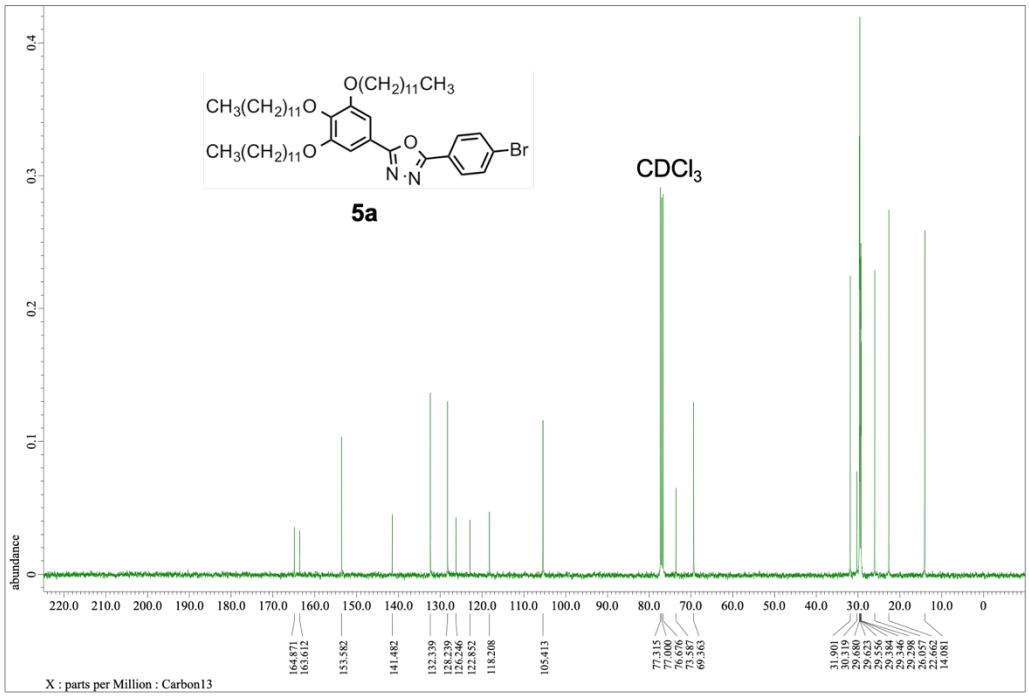

Figure S4. ^{13}C NMR spectrum of **5a** in $CDCl_3$ at 298 K.

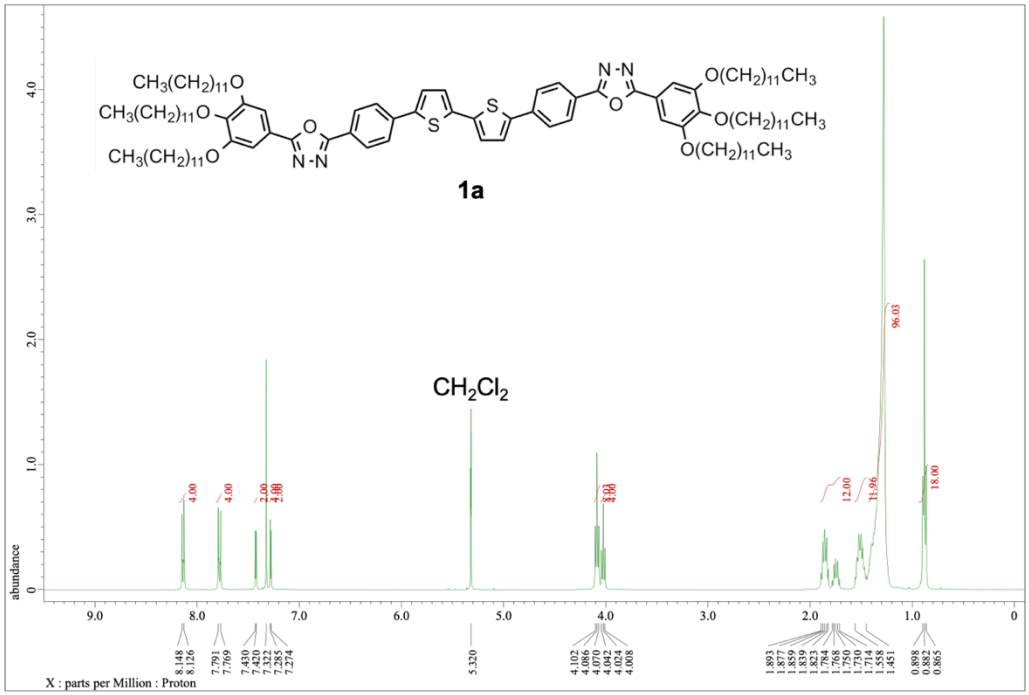

Figure S5. ^{1}H NMR spectrum of **1a** in CD_2Cl_2 at 298 K.

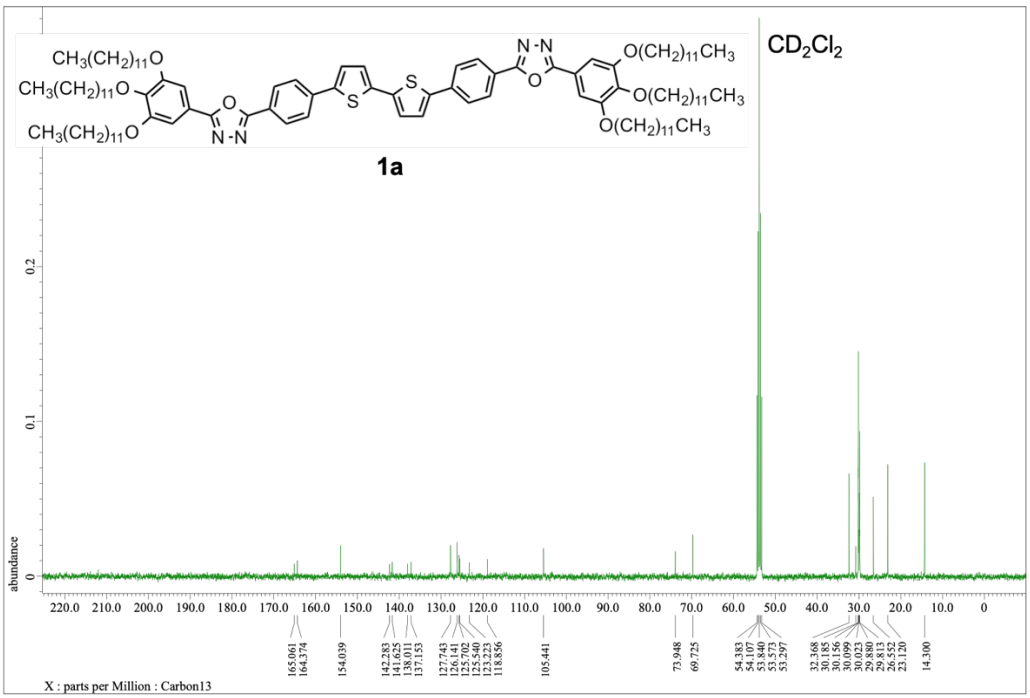

Figure S6. ^{13}C NMR spectrum of **1a** in CD_2Cl_2 at 298 K.

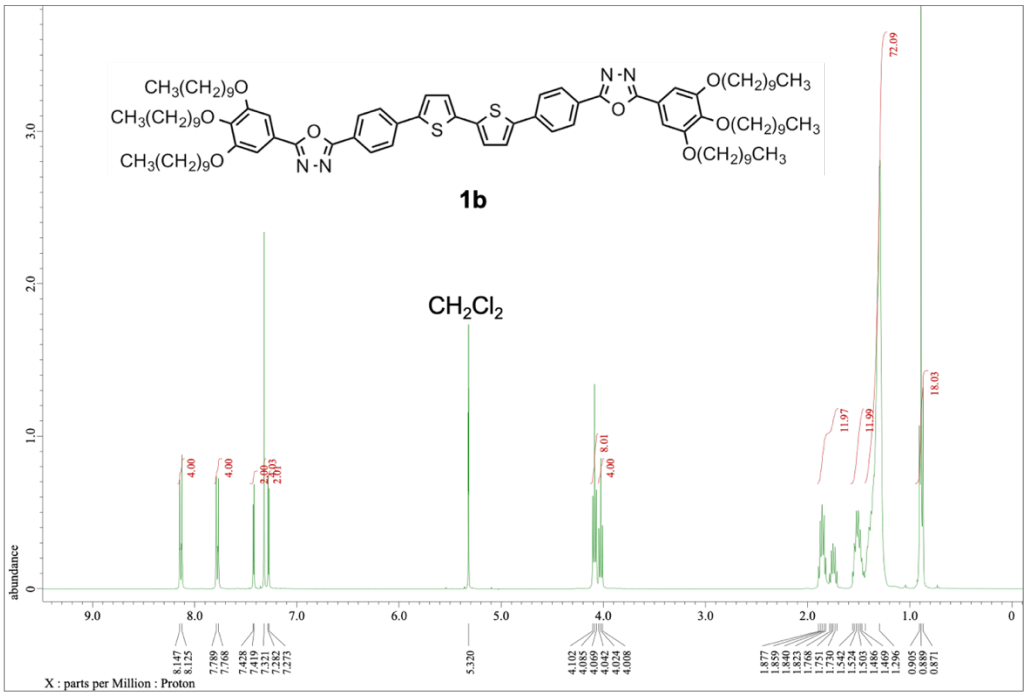

Figure S7. ^{1}H NMR spectrum of **1b** in CD_2Cl_2 at 298 K.

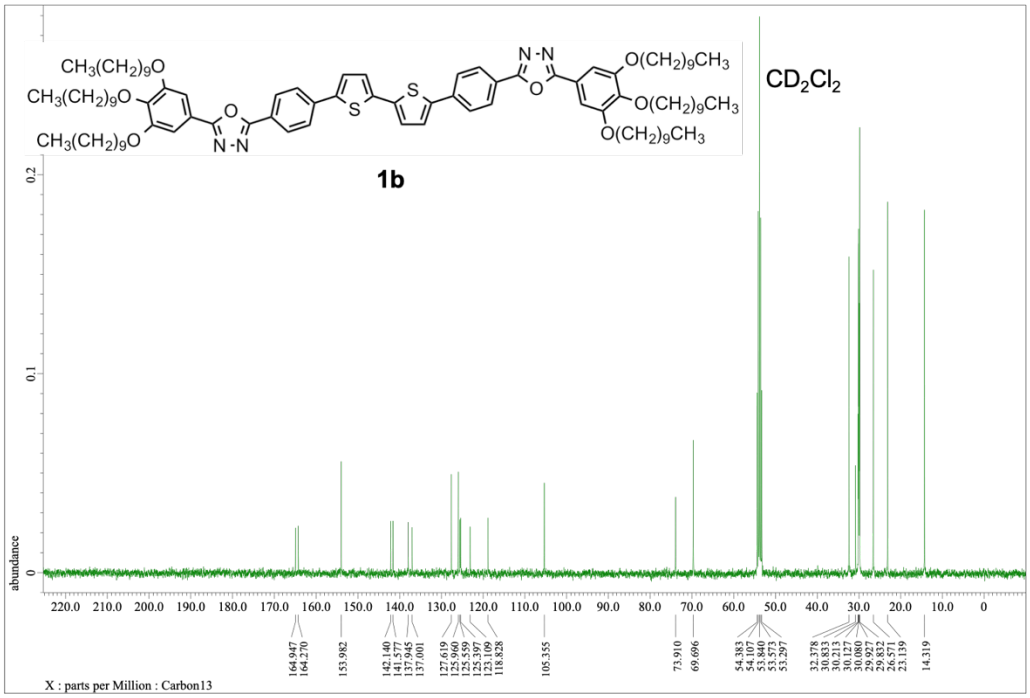

Figure S8. ^{13}C NMR spectrum of **1b** in CD_2Cl_2 at 298 K.

4. Electron density map

The electron density map was plotted for an LC sample of **1a** heated to 115 °C. First, we indexed the XRD peaks and deduced the lattice constants as $a = 4.26$ nm, $b = 2.83$ nm, and $\gamma = 80°$. Then we took an inverse Fourier transform from reciprocal space to the real space, using the determined lattice constants as $\boldsymbol{k}$ vectors and XRD peak intensities as Fourier coefficients.[S2] Peak phases were set to zero.

5. Liquid-crystalline properties

In DSC measurements, the sample was first heated to 170 °C, that is, above the isotropic liquid (Iso) temperature and then cooled to –30 °C. The second heating cycles are presented in Figure S9. By combining DSC, optical microscopy and XRD measurements, the thermal phase transitions were determined as follows. The transition temperatures were taken at onset, in °C, and the numbers in brackets are the corresponding enthalpies in kJ/mol.

1a: Crystal_1 (35) 67 || Crystal_2 105 || (37) LC 121 (33) || Iso

1b: Crystal_1 50 (5) || Crystal_2 66 (8) || Crystal_3 100 (17) || LC 125 (38) || Iso

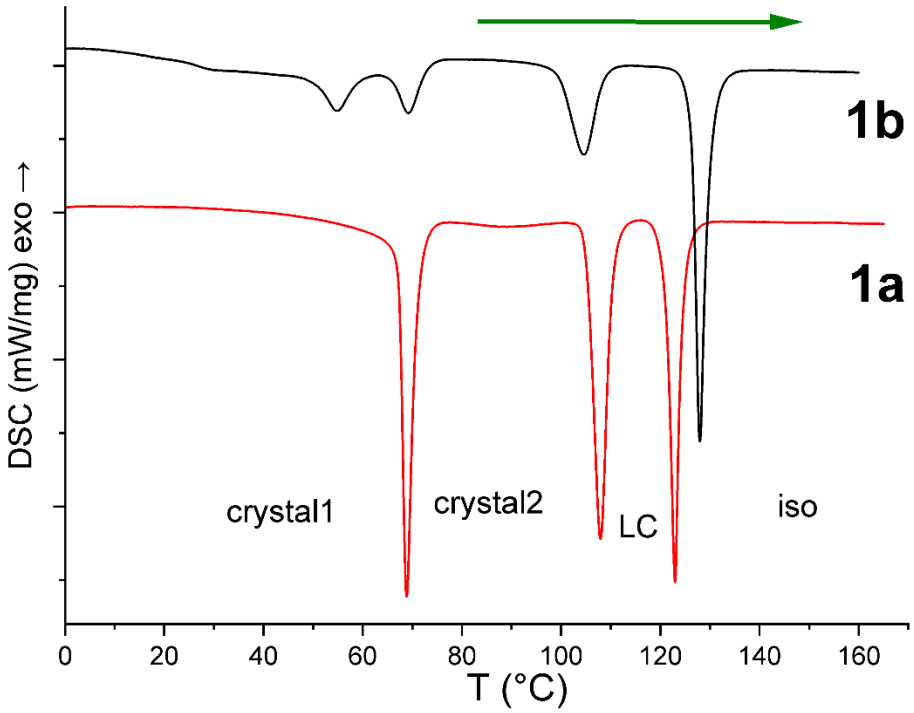

Figure S9. DSC thermographs of **1a** and **1b** recorded upon second heating. $\text{Crystal}_{1,2,3}$: crystalline phases, LC: columnar phase, Iso: isotropic liquid phase.

Liquid crystallinity was observed under a crossed Nicol's condition in a polarized optical microscope, and representative LC textures at 115 °C are shown in Figure S10. Figure S11 depicts the changes in LC textures before and after shearing.

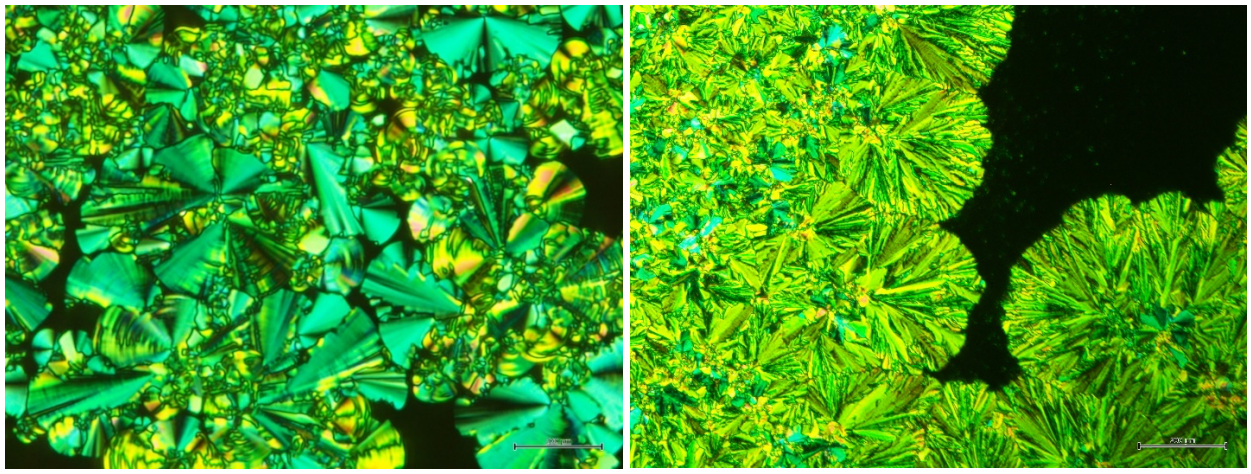

Figure S10. Representative optical textures of **1a** (left) and **1b** (right) in the LC state observed under crossed polarizers at 115 °C. Scale bar is 200 microns.

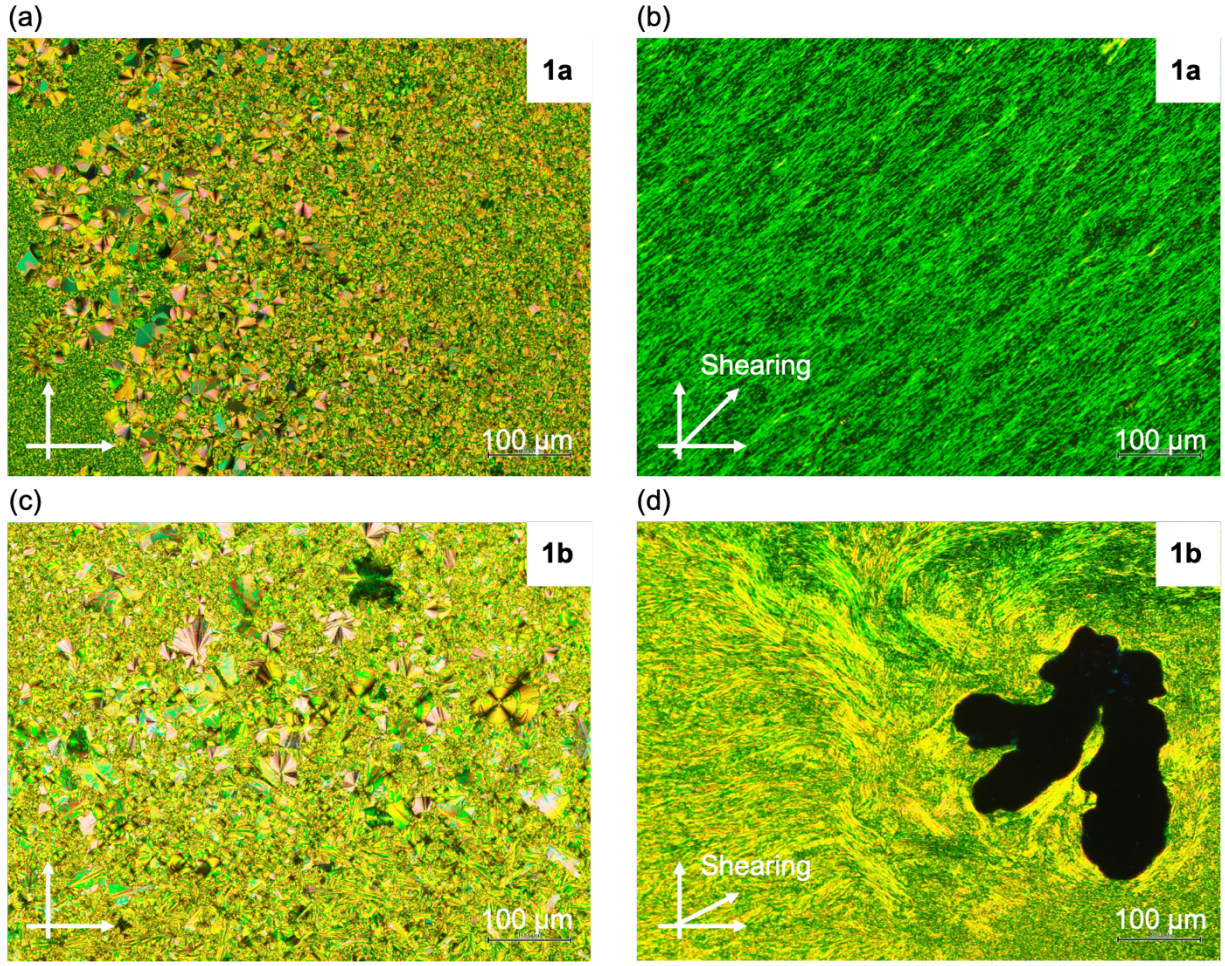

Figure S11. Polarized optical microscopic images of **1a** (a) before and (b) after shearing at 115 °C and **1b** (c) before and (d) after shearing at 120 °C.

6. Molecular structure drawn with Spartan 18

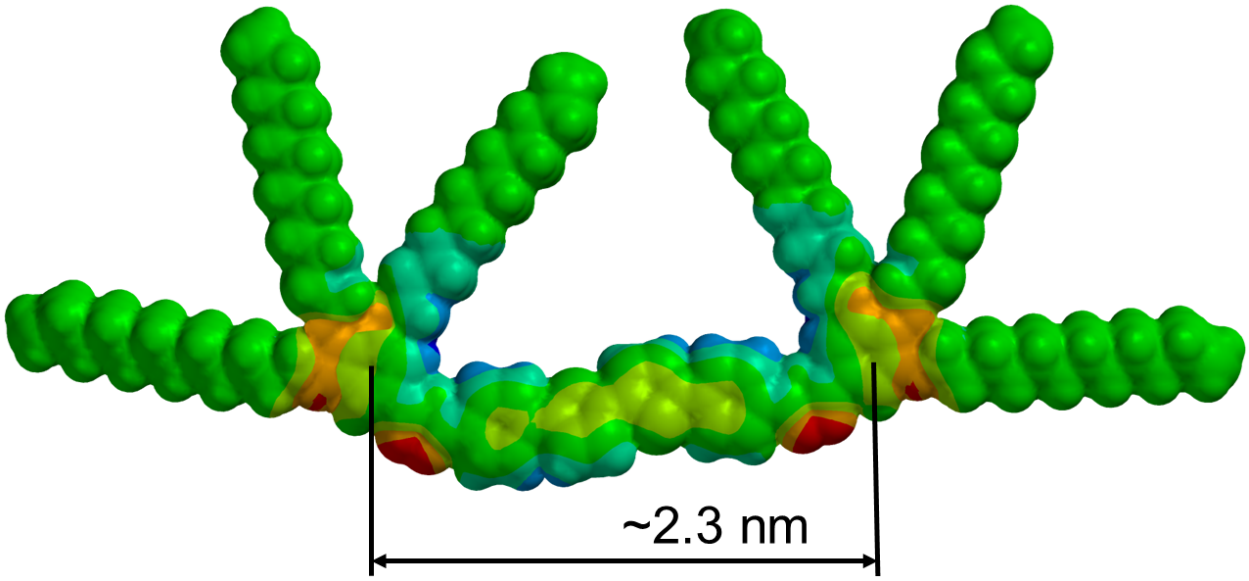

Figure S12. Electron density map of **1a** calculated by density functional theory using the Spartan 18 software. The density is represented by the spectral colors, and its value increases from blue to red.

7. Preparation and characterization of photoelectrical devices

We have used commercial sandwich cells (EHC, Japan) consisting of two glass plates separated by a 2 μm spacer. The inner glass surfaces were coated with nm-thick transparent indium tin oxide (ITO), which served as electrical contacts. In the central 4×4 mm squares, the bottom and top contacts overlapped, forming a sandwich cell (see the left panel of Figure S13).

Approximately 2 mg of **1a** or **1b** was placed at the open edge of an empty cell, which was then heated to 140 °C overnight. Melted material was sucked inside the cell by capillary force, filling up the space between ITO electrodes. Then the cell was cooled down to room temperature within an hour.

Alternating current impedance measurements were carried out using an Autolab PGSTAT128N impedance analyzer (Metrohm Autolab B.V., the Netherlands). An empty cell was used as a reference sample; its capacitance impedance and the value of capacitance did confirm the cell geometry specified by the manufacturer. The frequency range was 10^{7}–10^{-1} Hz and the applied voltage was 0.7 V. These measurements yielded the device capacitance and hence the low-frequency dielectric constant.

Dark current and photocurrent were measured with an Agilent B2900 source/measure unit. AM1.5 illumination was provided by the HAL-C100 Solar Simulator (Asahi Spectrum, Japan), and its intensity was verified by a factory-calibrated BS-520BK solar detector (Bunkoukeiki, Japan).

As-prepared samples exhibited symmetrical and nonlinear I-V curves, with a dark current of ca. 1 nA, a photocurrent of ca. 1 μA at 20 V and zero short-circuit photocurrent I_{SC}. However, after

the cell was "poled", that is, heated to above 105 °C while applying a DC voltage of 40 V (i.e. 20 V/μm), and then cooled down to room temperature within one hour, the following changes were observed (see Fig. 3 in the main text):

- A strong asymmetry in I-V curves, both in the dark and illuminated states; the sign of the asymmetry could be reversed by reversing the sign of applied voltage during the poling.
- A large increase in photocurrent, which was accompanied by the emergence of photovoltaic response with $I_{SC} \sim 0.35$ μA and open-circuit voltage $V_{OC} \sim 1$ V.
- An increase in the low-frequency (kHz) dielectric constant from 2.0 to 2.7.
- An increased optical transparency of the electrode area, which indicates that some molecules, or their constituents, have aligned normal to the electrodes thereby reducing their interaction with the electric field of incident light, which is oriented in the electrode plane.

Poling-induced changes were stable for at least several weeks, but they could be erased by a brief heating the sample to 120 °C without applied electric field.

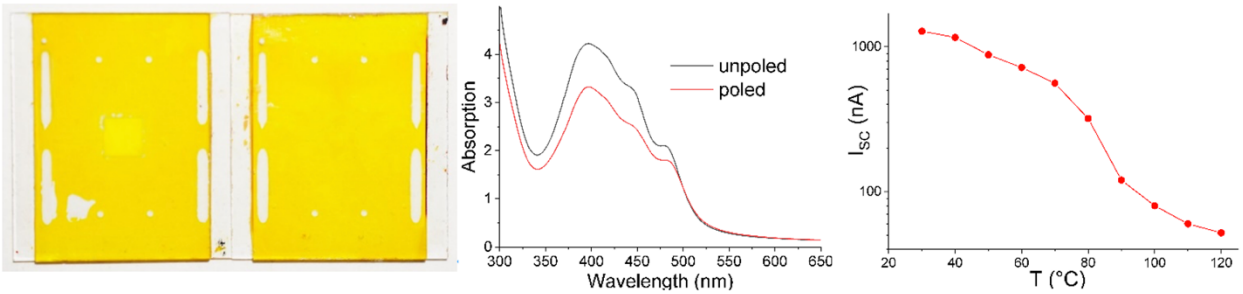

Figure S13. Characterization of **1a** devices. *Left*: Photographs of poled (left) and unpoled (right) cells. The central light-yellow square in the left cell corresponds to the 4×4 mm ITO electrodes. *Center*: Absorption spectra of the central regions. *Right*: Temperature dependence of the short-circuit current.

8. Luminescence measurements

Phosphorescence and most of luminescence spectra were recorded with an FP-8300 spectrometer (Jasco, Japan) using for excitation either an external laser or a built-in 150 W continuous-wave (CW) Xe lamp filtered by a single-grating monochromator. Emission was detected at 90° angle with respect to excitation beam. Phosphorescence spectra were measured using built-in light choppers that were synchronized with the detection electronics by the spectrometer hardware and software.

High-speed luminescence measurements were performed by recording either videos with an α6400 camera (Sony, Japan) at 120 frames/second or spectra with a SEC2020 spectrometer (ALS, Japan). The spectrometer is equipped with a Si CCD that can be synchronized with an external light source and can record spectra in the 200–1025 nm range within 1 ms.

Two-photon fluorescence was excited either by a pulsed Q-switched Nd-doped yttrium aluminium garnet laser (YAG:Nd; Continuum Minilite II, Amplitude, Japan), which provided 1-10 mJ, 5 ns pulses at 1064 nm with a frequency of 1–10 Hz, or by an 860 nm CW semiconductor laser with an in-focus intensity of 10 kW/cm^2.

We did not observe any significant variation in luminescence intensity from the solutions of **1a** or **1b** when using solvents with different polarity, such as chloroform and toluene.

White LED simulations (see Figure 6 in the main text) were performed as follows: the YAG:Ce phosphor was removed from a commercial white LED, yielding a low-power 450 nm LED. This LED was used for exciting luminescence from a thin film of **1a**, **1b** or the YAG:Ce phosphor. Luminescence was detected using the Si CCD spectrometer.

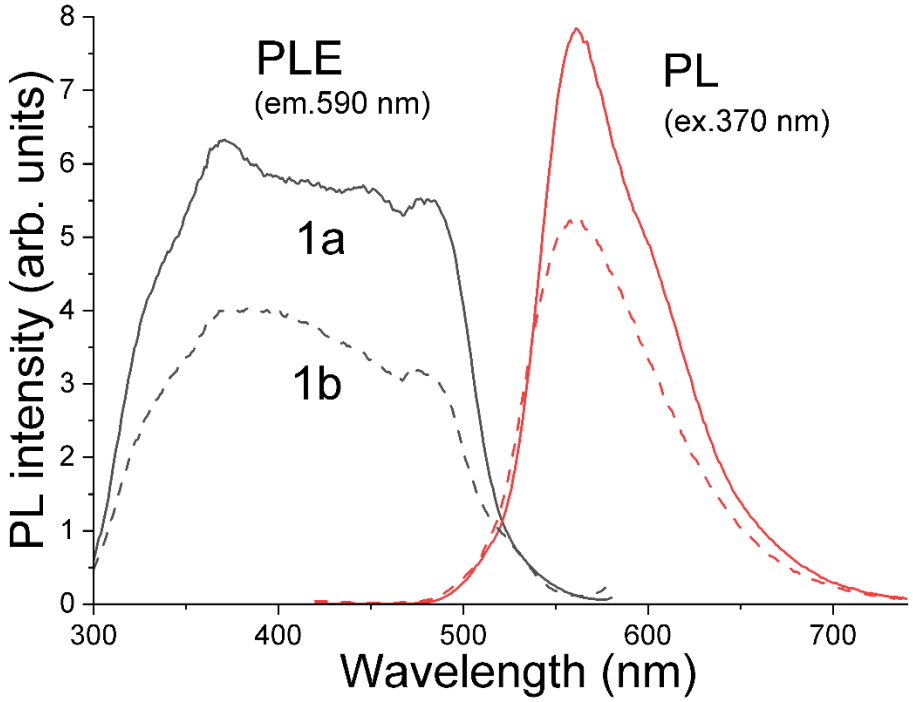

Figure S14. Room-temperature luminescence excitation and emission spectra of 2-micron-thick films of **1a** and **1b** measured at the same conditions.

9. References

[S1] S. Mondal, P. Chakraborty, P. Bairi, D. P. Chatterjee, A. K. Nandi, *Chem. Commun.*, 2015, **51**, 10680–10683.

[S2] M. Impéror-Clerc, *Interface Focus*, 2012, **2**, 589–601.